Journal of Hydrology 513 (2014) 322–334

Contents lists available at ScienceDirect

Journal of Hydrology

journal homepage: www.elsevier.com/locate/jhydrol

Incorporating the effects of increased atmospheric CO_2 in watershed model projections of climate change impacts

Jonathan B. Butcher [a,*], Thomas E. Johnson [b], Daniel Nover [c,1], Saumya Sarkar [a]

[a] Tetra Tech, Inc., PO Box 14409, Research Triangle Park, NC 27709, United States
[b] U.S. Environmental Protection Agency, Office of Research and Development, Washington, DC, United States
[c] U.S. Agency for International Development, West African Regional Office, Accra, Ghana

ARTICLE INFO

Article history:
Received 3 October 2013
Received in revised form 25 February 2014
Accepted 31 March 2014
Available online 12 April 2014
This manuscript was handled by Konstantine P. Georgakakos, Editor-in-Chief, with the assistance of Emmanouil N. Anagnostou, Associate Editor

Keywords:
Climate change
Evapotranspiration
CO_2
HSPF
SWAT
Stomatal conductance

SUMMARY

Simulation models such as the Hydrologic Simulation Program – FORTRAN (HSPF) and Soil–Water Assessment Tool (SWAT) are frequently used to project the responses of watershed processes to climate change, but do not always represent the effects of changes in atmospheric CO_2 concentrations on plant growth. Projected increases in atmospheric CO_2 concentrations may decrease the need for plants to maintain stomatal conductance to achieve sufficient CO_2 inputs, thereby also reducing the transpiration of water with potentially important effects on watershed water balance. We first compare the SWAT model, which provides an option to explicitly represent the effects of increased CO_2 to implementations of the SWAT model without this option and to the HSPF model, which does not include a representation of CO_2 response. Both models are capable of representing watershed responses to current climatic conditions. For analysis of response to future conditions, the SWAT model with integrated plant growth response to increased CO_2 predicts an increase in streamflows relative to models without the CO_2 response, consistent with previous research. We then develop methods to incorporate CO_2 impacts on evapotranspiration into a physically based modeling framework, such as HSPF, that does not explicitly model plant growth. With these modifications, HSPF also projects an increase in future runoff relative to simulations without accounting for the CO_2 effect, although smaller than the increase predicted by SWAT with identical assumptions for stomatal conductance. The results suggest that, while the effect of reduced plant transpiration due to increased atmospheric CO_2 is important, it is likely to be overestimated by both the current formulation of the SWAT model and modified versions that reduce the stomatal conductance response for woody plants. A general approach to modifying watershed models to simulate response of plant transpiration to increased atmospheric CO_2 under climate change is also proposed.

1. Introduction

There is growing concern about the potential effects of climate change on water resources. During the last century, human-influenced greenhouse gas emissions have resulted in regionally variable increases in temperature and changes in precipitation amount and intensity (IPCC, 2007; Karl et al., 2009). These trends are anticipated to continue and accelerate in the next century. While the details of future climate are uncertain, the range of likely changes presents a tangible risk to water resources due to projected changes in the volume and seasonal distribution of freshwater flows, potential changes in the intensity of hydrologic processes, and impacts of changed hydrology on the delivery and fate of sediment and pollutants (IPCC, 2007; Karl et al., 2009). Scenario analysis using watershed models is useful for understanding vulnerability to a range of potential changes. Given the complexity of simulating future climate, it is common practice to evaluate a range of future outcomes based on multiple scenarios developed using different climate models (e.g., Lopez et al., 2009; Elsner et al., 2010; Hay et al., 2011). Projecting watershed response to climate change presents a number of additional challenges. For example, with increasing precipitation, runoff is likely to increase; while, with increasing air temperature, evapotranspiration (ET) is likely to increase. If both precipitation and air temperature change, the net effect will be a balance between competing processes and more difficult to deduce from first principles.

* Corresponding author. Tel.: +1 919 485 2060.
E-mail addresses: jon.butcher@tetratech.com (J.B. Butcher), Johnson.Thomas@epa.gov (T.E. Johnson), dmnover@gmail.com (D. Nover), sam.sarkar@tetratech.com (S. Sarkar).
[1] Formerly at USEPA Office of Research and Development.

http://dx.doi.org/10.1016/j.jhydrol.2014.03.073
0022-1694/

Projections based on watershed models with different structures could influence or add variability to results. To date, the literature contains extensive discussion of the uncertainty in climate model projections and its propagation into watershed model projections, but relatively little on the effects of watershed model formulation on the results (although see Jiang et al., 2007 and Najafi et al., 2011). This paper examines how the different representations of ET in two comprehensive watershed management models in common use: the Soil Water Assessment Tool (SWAT; Arnold et al., 1998; Neitsch et al., 2005) and Hydrological Simulation Program – FORTRAN (HSPF; Bicknell et al., 2005), influence simulation results.

Evapotranspiration (ET) is a dominant term in the terrestrial hydrologic cycle, accounting for about 60% of precipitation, on average, across the globe (Shiklomanov, 1998), and consists of transpiration by plants and evaporation from soil and free water surfaces, including water temporarily stored in canopy and surface retention. Both evaporation and transpiration are driven by thermal energy and vapor pressure gradients. Projections of future climate include increased air temperature in most locations. Globally, air temperature is expected to increase on average faster than relative humidity resulting in increased ET. The average rate of ET is expected to increase by about 6.8% for each 1 °C increase in air temperature (Katul et al., 2012). Changes in ET cause changes in streamflow, which in turn affect stream water quality, including loads of nitrogen, phosphorus, and sediment.

Anthropogenic emissions of CO_2 are a primary contributor to global warming (IPCC, 2007). In addition to changes in climate, there are also direct effects of increased atmospheric CO_2 on hydrology. Changes in CO_2 concentration affect plant growth and physiology, resulting in changes in ET, watershed biogeochemistry, and water balance. To evaluate future conditions, it is important to consider the direct effects of increased CO_2 together with the effects of climate change. (Hereafter, we use the shorthand "future climate" to mean climate together with the changes in CO_2 that contribute to climate change.) IPCC estimates of future atmospheric CO_2 concentrations project an increase from 369 ppmv CO_2 in 2000 to about 532 ppmv (using the ISAM model reference run) or 522 ppmv (using the Bern-CC model reference run) in 2050 (Appendix II in IPCC, 2001), with a median of 527 ppmv, under both the A2 and A1B emissions storylines, which diverge after 2050. Plants require CO_2 from the atmosphere for photosynthesis. An important effect of elevated atmospheric CO_2 is decreased stomatal conductance, as plants require less time with open stomata to support the inward diffusion of CO_2 needed for growth, thus reducing leaf loss of water (Field et al., 1995). This effect can potentially counterbalance projected increases in temperature and potential evapotranspiration (PET). It may also reduce water stress on plants, resulting in greater biomass and litter production, which in turn will influence pollutant loads.

In the past it has been argued that these responses of plants to increased CO_2, long documented at the leaf and organism level, might not translate to true ecosystem effects. However, recent research, particularly the Free-Air CO_2 Enrichment (FACE) experiments summary (Leakey et al., 2009) suggests that significant ET reductions do occur at the ecosystem level under elevated CO_2 – although there are differences in responses among plant species, with lesser effects reported for some conifers than in agricultural crops (Field et al., 1995). The landscape-scale magnitude of the response to CO_2 levels projected by the mid-21st century varies in different experiments (Katul et al., 2012), but can be on the order of a 10% reduction in ET response (Bernacchi et al., 2007). Further, a recent study by Cao et al. (2010) suggests that up to 25% of the temperature increase projected for North America could result directly from decreased plant ET under increased CO_2 concentrations. Lammertsma et al. (2011) summarize paleoecological evidence that stomatal density has decreased over the past 150 years in Florida vegetation, apparently in response to rising CO_2. However, the actual response to future climates may be limited by interactions with other biogeochemical factors. For instance, Reich et al. (2006) point out that the response to elevated CO_2 is reduced when soil N supply is low and, in turn, elevated CO_2 may suppress net N mineralization and plant availability in soil.

Watershed models can be used to simulate the effects of the changing climate, including changes in atmospheric CO_2, on water quantity and quality; however, the results are conditional on the structure of the model used. Watershed models that do not explicitly model plant growth responses, such as HSPF, may omit significant impacts of changes in plant growth and physiology on the water balance. Several studies have used SWAT, which includes a plant growth model that represents the CO_2 effect on ET, to demonstrate that increased CO_2 will likely result in higher streamflow than would be expected from changes in precipitation and PET alone, using both the standard version of SWAT (Jha et al., 2006; Ficklin et al., 2009; Van Liew et al., 2012) and modified versions with enhanced representation of the stomatal conductance effect (Eckhardt and Ulbrich, 2003; Wu et al., 2012a,b; Luo et al., 2013).

This paper compares the projected effects of climate change on streamflow and water quality using SWAT and HSPF with and without representation of increased atmospheric CO_2. As HSPF does not explicitly model plant growth and thus does not have a native capability for representing effects of atmospheric CO_2 on plant growth and therefore on the water balance, this paper also presents an approach to incorporate CO_2 impacts on ET into HSPF or similar models. Creating a version of HSPF consistent with SWAT in terms of CO_2-mediated stomatal conductance effects on ET reveals other fundamental differences between the two models that affect the prediction of response to future climate.

2. Study areas

This work is based on simulations of watershed response to global change for five study areas that we performed as part of a larger modeling effort (Johnson et al., 2012; USEPA, 2013). These study areas, at approximately the 4-digit USGS hydrologic unit code (HUC; Seaber et al., 1987) scale (29,000–71,000 km^2), span a range of geographic, hydroclimatic, physiographic, and land use conditions: the Apalachicola–Chattahoochee–Flint (ACF) river basins in Georgia, Alabama, and Florida; the Minnesota River basin in Minnesota and South Dakota; the Salt–Verde–San Pedro river basins in Arizona; the Susquehanna River basin in Maryland, Pennsylvania, and New York; and the Willamette River basin in Oregon (Fig. 1 and Table 1). Sampling over watersheds with a range of settings is important to test different aspects of model performance. The five study areas represent a variety of climate characteristics, ranging from dry (Arizona) to wet (Willamette) and from cool (Minnesota) to warm (ACF). Row crop agriculture is near zero in the Arizona basins, but occupies over 72% of the watershed area in the Minnesota River. Winter runoff is dominant in the Willamette, while summer runoff is dominant in the Minnesota River basin.

3. Methods

Watershed modeling was conducted in each of the five study areas using two different watershed models: HSPF and SWAT. These models were selected because they are dynamic simulation models that are able to simulate water quality responses, are in the public domain, and are widely used and accepted for water quantity and quality planning applications in the U.S. (Duda et al., 2012; Gassman et al., 2007). The HSPF and SWAT model pairs for each

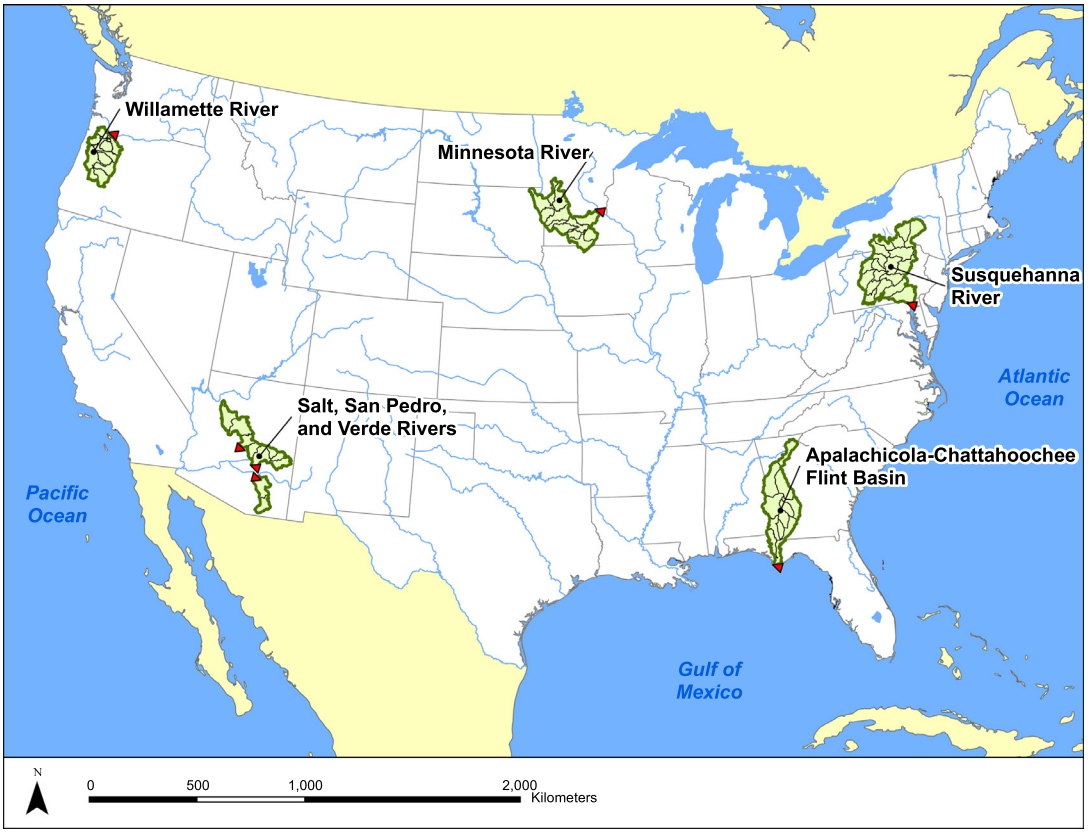

Fig. 1. Study areas.

Table 1
Model study areas.

Study area	Total area (km^2)	Elevation range (m MSL)	Average precip (cm/yr)	Average temp (°C)	Percent row crop (%)	Percent urban land (%)	Percent forest (%)	Ratio winter to summer runoff	Fraction of runoff as snowmelt (%)
Apalachicola–Chattahoochee–Flint (ACF)	49,943	0–1325	138	17.5	12.4	9.3	47.9	2.01	0.7
Arizona: Salt, Verde, and San Pedro	38,617	585–429	50	13.8	0.1	1.2	41.9	2.06	9.3
Minnesota River	44,001	208–650	72	6.6	72.1	6.6	2.9	0.50	14.8
Susquehanna River	71,235	0–957	105	9.0	9.8	7.4	61.1	2.06	16.6
Willamette River	29,031	0–3185	148	10.7	8.2	7.2	56.2	10.99	4.5

Notes: Precipitation and temperature are averages over the weather stations used in simulation for the modeling period (approximately 1970–2000, depending on study area). The ratio of winter (January–March) to summer (July–September) runoff and the fraction of runoff as snowmelt are derived from the calibrated SWAT model applications described in USEPA (2013).

study area were calibrated independently by the first author and six others (listed in the Acknowledgments) using a common protocol.

The models were applied to simulate the watershed response to a range of potential mid-21st century changes in climate (Johnson et al., 2012). The six primary future scenarios are based on mid-21st century climate model projections downscaled with six regional climate models (RCMs) applied to four GCMs from the North American Regional Climate Change Assessment Program (NARCCAP). The models were also run using four mid-21st century scenarios relying on the same GCMs from the bias-corrected and spatially downscaled (BCSD) data set described by Maurer et al. (2007) and four scenarios based on non-downscaled GCMs for an investigation of the impacts of downscaling methodology described in USEPA (2013).

The model scenarios were used to evaluate projected streamflow and water quality (total suspended solids [TSSs], total phosphorus [TP], and total nitrogen [TN] loads) for different modeling options. SWAT (with representation of increased atmospheric CO_2 impacts) and HSPF (without representation of increased CO_2) are compared in all 5 study areas, as are SWAT projections with and without representation of increased CO_2. After modifying the HSPF model, comparisons of HSPF projections with and without representation of increased atmospheric CO_2, and comparisons of SWAT and HSPF projections with representation of increased CO_2 are undertaken in two study areas with different climate

characteristics (Table 1) – the ACF (warm, humid) and the Minnesota River (cool, continental).

3.1. Watershed models

HSPF and SWAT have different structures and algorithms, resulting in different strengths and weaknesses. The following sections describe the key components of each model.

3.1.1. HSPF

HSPF (Bicknell et al., 2005) is a comprehensive watershed and receiving water quality modeling framework developed with support from the U.S. Environmental Protection Agency (EPA) and U.S. Geological Survey. During the past several decades, it has been used to develop hundreds of EPA-approved Total Maximum Daily Loads (TMDLs), and it is generally considered among the more advanced hydrologic and watershed loading models available (Duda et al., 2012).

The hydrologic portion of HSPF is based on the Stanford Watershed Model (Crawford and Linsley, 1966). The water balance is simulated based on Philip's infiltration (Bicknell et al., 2005) coupled with multiple surface and subsurface stores (interception storage, surface storage, upper zone soil storage, lower zone soil storage, active groundwater, inactive [deep] groundwater).

Sediment processes in HSPF consider detachment by rainfall or mechanical disturbance, deposition, and gullying processes, coupled with transport capacity based on overland flow. Upland nutrient loads may be simulated at varying levels of complexity, but are most typically represented by either buildup/washoff or sediment potency approaches on the land surface coupled with user-specified monthly concentrations in interflow and groundwater.

Spatially, the watershed is divided into a series of sub-basins representing the drainage areas that contribute to each of the stream reaches. The stream module links the surface runoff and groundwater flow contributions from each of the land segments and sub-basins and routes them through the waterbody network. HSPF is typically implemented in large watersheds at an hourly time step.

HSPF, as currently formulated, is not able to directly simulate effects of increased CO_2 on ET. Instead, time series of PET and monthly coefficients that control exertion of PET on soil moisture for each land cover are supplied by the user. The version of HSPF used in this study is WinHSPF as distributed with BASINS ("Better Assessment Science Integrating point & Non-point Sources") version 4.0 (USEPA, 2009).

3.1.2. SWAT

SWAT (Arnold et al., 1998) was developed by the U.S. Department of Agriculture to simulate the effect of land management practices on water, sediment, and agricultural chemical yields in large, complex watersheds with varying soils, land use, and management conditions over long periods of time. SWAT requires data inputs for weather, soils, topography, vegetation, and land use to model water and sediment movement, nutrient cycling, and numerous other watershed processes. SWAT is a continuous model appropriate to long-term simulations. SWAT version 2005 (Neitsch et al., 2005) was used in this study.

SWAT can use either a curve number approach or Green–Ampt infiltration to estimate surface runoff, then completes the water balance through simulation of subsurface flows, ET, change in soil storages, and deep seepage losses. The majority of SWAT applications use the curve number approach (Gassman et al., 2007), which requires a daily time step. PET is typically calculated internally by SWAT based on other weather inputs.

Sediment yield and erosion are calculated by SWAT using the Modified Universal Soil Loss Equation (MUSLE; Williams, 1975). Nutrient load generation and movement are simulated as a function of overland runoff and subsurface flow. The transformation of various nitrogen and phosphorus species is simulated in detail in the soil; however, concentrations of nutrients in groundwater discharges are user-specified in this version, as is done in HSPF when nutrient loads from upland segments are simulated as general quality constituents. As in HSPF, a stream simulation links the surface and subsurface contributions from each of the land segments and routes them through the waterbody network.

SWAT incorporates an explicit plant growth model, including plant interactions with water, nutrient stores, and atmospheric CO_2. SWAT allows the user to simulate the effect of changes in CO_2 concentration on plant stomatal conductance and resulting impacts on ET using the method Easterling et al. (1992) (see Section 4.1). SWAT also simulates the change in radiation use efficiency of plants as a function of CO_2 concentration using the method developed by Stockle et al. (1992).

3.2. Model setup

HSPF and SWAT are semi-distributed models in which the study area is divided into subbasins and land segments within each subbasin are simulated on a unit area basis. Both models were implemented using a hydrologic response unit (HRU) approach to upland simulation. An HRU consists of a unique combination of land use/land cover, soil, slope, and land management practice characteristics, and thus represents an area of similar hydrologic response. This is the default for SWAT, but is also good practice with HSPF. Individual land parcels represented as an HRU are expected to possess similar hydrologic and load generating characteristics and can thus be simulated as a unit.

The SWAT application was set up using ArcSWAT (Winchell et al., 2008). Subbasin boundaries and reaches were defined from the National Hydrography Dataset Plus (NHDPlus) catchments (USEPA, 2010), aggregated to approximately the HUC 10-digit scale. The subbasin and reach shapefiles were imported into the SWAT interface and subbasin parameters were calculated automatically.

Land cover data for the model come from the 2001 National Land Classification Dataset (NLCD), version 1 (Homer et al., 2004, 2007). Consistent with the broad spatial scale of the models, the land cover component of the HRUs is interpreted to a relatively small number of categories (e.g., forest, wetland, range, grass/pastureland, crop, developed pervious, low-density developed, and high-density developed). Impervious percentage was assigned to developed land use classes in the SWAT urban database using values calculated from the NLCD impervious coverage.

Soils data are from the STATSGO state soils coverage (USDA, 1991) distributed with ArcSWAT. The soils coverage was assigned using the dominant component method in which each soil polygon is represented by the properties of the dominant constituent soil in STATSGO. Elevations and slopes are taken from the National Elevation Dataset at a resolution of 30 m (Gesch et al., 2002). Slopes were classified in two categories with a breakpoint at 10%. A single breakpoint was chosen to represent major differences in runoff and erosive energy without creating an unmanageable number of individual HRUs.

HRUs were created by overlaying land use, soil, and slope at appropriate cutoff tolerance levels to prevent the creation of large numbers of insignificant HRUs: Land use classes were retained if they occupied at least 5% of the area of a subbasin (with the exception of developed land uses, which were retained regardless of area); soils were retained if they occupied at least 10% of the area within a given land use in a subbasin; and slope classes were retained if they occupied at least 5% of the area within a given soil polygon. Land uses, soils, and slope classes in which percent area

falls below the cutoff value are reapportioned to the dominant classes so that 100% of the watershed area is modeled (Winchell et al., 2008). Elevation bands with appropriate lapse rates were turned on to account for orographic effects in areas with significant elevation changes.

Next, land management operations were assigned, primarily to account for agricultural practices. For urban lands, the USGS regression method for pollutant load estimation was specified. In-stream water quality options started with SWAT defaults, which include simplified representations of channel scour and deposition, nutrient kinetics, and algal growth. Only those permitted point sources identified as major facilities (greater than 1 MGD discharge) were included in the model.

The HSPF models were developed from the same spatial coverages used to set up the SWAT models. The model segmentation is identical for the two models. The HRUs for HSPF were calculated from the SWAT HRUs, but differ in that soils were aggregated to NRCS hydrologic soil group, while pervious (PERLND) and impervious (IMPLND) land fractions were specified separately, consistent with standard practice for HSPF (USEPA, 2000).

Setup of the HSPF model used the WinHSPF interface to create the user control input (UCI) and watershed data management (WDM) files. Initial parameter values were based on previous HSPF modeling where available. For areas without previous modeling, hydrologic parameters were based on recommended ranges in USEPA (2000) and related to soil and meteorological characteristics where appropriate. Snowmelt simulation used the simplified degree-day method.

The stage–storage–discharge hydraulic functional tables (FTables) for stream reaches were generated automatically during model creation. The WinHSPF FTable tool calculates the tables using relationships to drainage area. FTables were adjusted in WinHSPF if specific information was available to the modeler. Hydraulic characteristics for major reservoirs and flow/load characteristics for major point sources were defined manually based on available information.

Nutrients on the land surface were modeled as inorganic nitrogen, inorganic phosphorus, and total organic matter. The latter was transformed to appropriate fractions of organic nitrogen and organic phosphorus in the linkage to the stream. The in-stream simulation represented total nitrogen and total phosphorus as general quality constituents (GQUALs) subject to removal approximated as an exponential decay process. Initial values for decay rates were taken from USGS SPARROW studies (e.g., Alexander et al., 2008).

The HSPF and SWAT models used a common set of 31 years of meteorological forcing data from multiple stations (approximately 50 per study area) commencing between 1969 and 1972 depending on data availability in the study area. Precipitation and air temperature time series (hourly for HSPF, daily for SWAT) were obtained from the BASINS meteorological data set (USEPA, 2008). Wind, relative humidity, and solar radiation, for which consistent 30-year time series are not available at many stations, were simulated using the SWAT weather generator (Neitsch et al., 2005; Allen et al., 1998). PET was calculated using the Penman–Monteith energy balance approach (Monteith, 1965) rather than simpler air temperature-based approaches to allow for the effects of potential future changes in the relationship between energy inputs.

3.3. Model calibration and validation

The modeling team calibrated and validated both of the models in each of the five study areas focusing at the HUC 8-digit scale (typically around 2000–3000 km^2), using the last 10 years for calibration and the prior 10 years for validation. Performance was evaluated relative to a variety of model fit statistics for streamflow and estimated monthly loads of nitrogen, phosphorus, and TSS, but this section focuses on the hydrologic fit based on total volume error and the monthly Nash–Sutcliffe efficiency (*E*, Nash and Sutcliffe, 1970). In each study area the initial calibration effort focused on a specific HUC 8-digit scale headwater gage within the overall HUC 4-digit scale study area, followed by adjustments to match streamflow at up to nine other gages in the watershed. Model performance is summarized for the focus calibration watershed followed by similar analyses for the largest-scale downstream watershed.

Summary results of calibration and validation are shown in Table 2, and full details are available in USEPA (2013). In general, the quality of fit was acceptable for both models. However, at the HUC 8-digit and larger scale, the fit in most of these watersheds is constrained by the presence of dams and other actively managed structures, which were represented in the model only by the target release method (in SWAT) or storage-discharge relationships (in HSPF) to allow application to altered climates. For many of the five study areas and multiple calibration points the quality of model fit tended to be slightly better (smaller relative error, larger *E*

Table 2
Summary hydrologic calibration and validation statistics (relative error on volume and monthly Nash–Sutcliffe efficiency).

Study area	Calibration gages	Model	HUC 8-digit focus, 10-yr calibration	HUC 8-digit focus, 10-yr validation	Downstream calibration (HUC 4-digit scale)
Apalachicola–Chattahoochee–Flint (ACF)	9	HSPF	5.5%	5.8%	16.8%
			0.93	0.92	0.83
		SWAT	7.3%	3.3%	16.5%
			0.91	0.90	0.82
Minnesota River	9	HSPF	1.6%	14.8%	−4.2%
			0.91	0.88	0.97
		SWAT	−5.4%	−0.8%	7.9%
			0.92	0.86	0.91
Arizona: Salt, Verde, San Pedro Rivers	10	HSPF	2.4%	6.3%	4.5%
			0.76	0.71	0.52
		SWAT	−2.5%	5.7%	9.4%
			0.70	0.67	0.46
Susquehanna River	3	HSPF	−0.2%	−8.0%	1.8%
			0.89	0.88	0.86
		SWAT	−5.4%	−16.3%	−9.7%
			0.67	0.66	0.64
Willamette River	5	HSPF	−3.9%	−9.8%	2.6%
			0.95	0.95	0.92
		SWAT	−4.7%	−12.2%	−5.0%
			0.95	0.86	0.89

Note: See USEPA (2013) for complete model calibration details.

coefficient) for the HSPF application. This is likely due in large part to the use of daily precipitation in SWAT versus hourly precipitation in HSPF, although the advantage accruing to HSPF is muted by the fact that many of the "hourly" precipitation input series used are actually disaggregated from daily totals. However, relative performance of the two models is more similar as the analysis moves to the validation period or to gages for which detailed calibration was not undertaken.

4. Theory: Representing effects of increased CO_2 on evapotranspiration

4.1. SWAT representation of evapotranspiration

SWAT allows several options for the representation of ET. We used the Penman–Monteith energy balance approach to evaluate the net response to changes in the full suite of meteorological variables. The Penman–Monteith option in SWAT also incorporates adjustments for the effects of increased CO_2 on plant growth and ET.

Penman (1948) developed an energy balance approach to estimating evaporation from a Class A evaporation pan. A full energy balance analysis of ET from plants takes a similar form, based on Monteith's (1965) insights into the use of the resistance concept to describe stomatal control over respiration. Under assumptions of well-watered plants, neutral atmospheric stability, and logarithmic wind profiles (Jensen et al., 1990), the form of the Penman–Monteith equation implemented by the SWAT model (Neitsch et al., 2005) is:

$$\lambda E_t = \frac{\Delta(R_n - G) + \gamma \cdot K_1 \cdot (0.622 \cdot \lambda \cdot \rho_{air}/P) \cdot (e_z^0 - e_z)/r_a}{\Delta + \gamma \cdot (1 + r_c/r_c)}, \quad (1)$$

in which λ is the latent heat of vaporization (MJ/kg), E_t is the maximum (non-water limited) evapotranspiration rate (mm/d), Δ is the slope of the saturation vapor pressure curve (which varies as a function of air temperature), R_n is the net radiation (MJ/m^2/d), G is the soil heat flux (MJ/m^2/d), K_1 is a unit conversion coefficient, γ is the psychrometric constant (as kPa/°C; varies as a function of elevation), ρ_{air} is the density of air (kg/m^3), P is the atmospheric pressure (kPa), e_z^0 is the saturation vapor pressure at elevation z (kPa), e_z is the actual vapor pressure at elevation z, r_a is the aerodynamic resistance (s/m), and r_c is the plant canopy (stomatal) resistance (s/m).

SWAT models the effect of changes in CO_2 concentration on plant stomatal conductance using the equation developed by Easterling et al. (1992), in which increased CO_2 leads to decreased leaf conductance, which in turn results in an increase in the canopy resistance term in the PET calculation. The model also simulates the change in radiation use efficiency of plants as a function of CO_2 concentration using the method developed by Stockle et al. (1992). The canopy resistance, r_{c1}, is represented as:

$$r_{c1} = r_l \cdot 1 \Big/ 0.5LAI \cdot \left(1.4 - 0.4 \cdot \frac{[CO_2]}{330}\right), \quad (2)$$

where r_l is the minimum effective stomatal resistance of a single leaf (s/m), LAI is the leaf area index, and $[CO_2]$ is the atmospheric concentration of CO_2 in ppmv. Note that Easterling et al. developed this equation relative to $[CO_2]$ concentration for the early 1990s of 330 ppmv, and adjustments may need to be made for a different baseline period.

Eq. (2) was developed for crop systems in the Missouri–Iowa–Nebraska–Kansas region and implies that a doubling of CO_2 concentration leads to a 40% decrease in stomatal conductance. Jha et al. (2006) acknowledged that the literature suggests a lower rate of decrease may be appropriate for some plants, especially certain tree species. Recently Wu et al. (2012a,b) proposed a more generalized form of the equation as

$$r_{c1} = r_l \cdot 1 \Big/ 0.5LAI \cdot \left((1 + p) - p \cdot \frac{[CO_2]}{330}\right), \quad (3)$$

where p is the decline in stomatal conductance at $[CO_2] = 660$ ppmv, and also introduced a modification that estimates change in leaf area in response to elevated CO_2. The evidence for a lower rate of decline in conductance is somewhat mixed. The review of Medlyn et al. (2001) reported changes in mean stomatal conductance in forest species in response to doubled CO_2 ranging from −1% to −24% with an overall mean effect of −21% under unstressed conditions; however, they also noted that effects were larger in longer (>1 yr) studies and under conditions of water stress (mean response of −31%; 95% confidence limits of −44% to −16%). The latter finding may be of particular significance for future climate conditions with elevated temperatures. In any event, we chose to retain the original SWAT formulation in this study as it is the form most likely to be applied by others – but note that the representation can readily be converted to the more flexible form of Wu et al. (2012a,b).

4.2. HSPF native implementation of evapotranspiration

HSPF does not include a plant growth model that can automatically respond to changes in CO_2 concentrations; however, the discussion in the previous section, as well as the results of model experiments reported below in Section 5, indicates that incorporating such responses is important. To plan how best to implement this adjustment it is useful to first discuss how HSPF handles ET.

In HSPF, time series of PET are an externally specified input to the model. PET is used to evaluate evaporative losses from impervious surfaces, from free water surfaces, and from pervious land units. The first two cases are straightforward. For pervious land units, both surface evaporation and plant transpiration are important. The model allocates potential evaporation from pervious land areas in the following order (Bicknell et al., 2005):

1. Active groundwater discharge to streams (up to the fraction of ET specified by the parameter *BASETP*).
2. Interception storage in the canopy.
3. Storage in the upper soil/litter zone (with the fraction removed depending on the ratio of current storage to nominal storage capacity of the upper zone).
4. Active groundwater storage in land units where the water table is at or above the surface, such as wetlands that are not simulated as waterbodies (up to the fraction specified by the parameter *AGWETP*).

Remaining PET is then applied to moisture storage in the lower soil zone (defined as the root zone of the soil profile), representing transpiration by rooted plants. The ET from the lower soil zone is modified by the parameter *LZETP*, which can vary throughout the year according to leaf area development. If *LZETP* was equal to one, representing near complete areal coverage of deep rooted vegetation with unlimited leaf area, then the potential ET for the lower soil zone is equal to the demand that remains after accounting for the higher priority sources listed above. However, this is usually not the case. Further, the actual ET can be limited by tension as water storage declines. HSPF represents this through use of an empirical approach in which the actual lower zone ET declines linearly to zero from a total remaining PET of *RPARM* and the maximum lower zone ET per simulation interval (when PET is not limiting) is calculated as

$$\text{Max(Lower Zone ET)} = \frac{RPARM}{2} = \frac{0.125}{1 - LZETP} \cdot \frac{LZS}{LZSN} \cdot \frac{DELT60}{24}, \quad (4)$$

where *LZS* is the current lower zone storage (depth), *LZSN* is the lower zone nominal storage parameter (depth), and *DELT*60 is the number of hours in a simulation interval. *LZETP* is restricted to the range of 0–1 and typically assigned within the range 0.1–0.9 (USEPA, 2000).

4.3. HSPF modifications to represent CO_2 effects on ET

Increased atmospheric CO_2 concentration will not directly alter the direct evaporation component of ET. Therefore, the PET time series itself should not be altered in HSPF to account for stomatal conductance effects. Instead, only the portion of ET calculated for the lower soil (root) zone in HSPF should be modified to reflect decreases in the transpiration component of ET. That is, the modification should be made through changes to the monthly values of the parameter *LZETP*.

An adjustment to *LZETP* to reflect a fractional change in actual ET (as a result of increased CO_2) can readily be calculated. Suppose τ is the ratio between actual ET calculated after accounting for increased CO_2 (AET_1) and that calculated without accounting for increased CO_2 (AET_0) under conditions when moisture is not limiting. Non-water limited conditions (consistent with the energy-balance analysis of actual ET developed by Monteith, 1965) imply that *LZS*/*LZSN* can be taken as constant and equal to 1, in which case:

$$\tau = \frac{\mathrm{AET}_1}{\mathrm{AET}_0} = \frac{1/(1 - LZETP_1)}{1/(1 - LZETP_0)} = \frac{1 - LZETP_0}{1 - LZETP_1} \tag{5}$$

Eq. (5) is rearranged to determine that $LZETP_1$ – the modified value of the parameter to achieve the ratio τ – should be set to

$$LZETP_1 = \mathrm{Max}\left\{1 - \frac{1 - LZETP_0}{\tau}, 0.1\right\}, \tag{6}$$

where 0.1 is an appropriate lower bound on *LZETP*.

4.4. Calculating the adjustment ratio

The key point from the perspective of evaluating the effect of increased CO_2 concentrations on ET is that AET varies as a function of $1/[\Delta + \gamma(1 + r_c/r_a)]$. To express the canopy resistance as a function of CO_2 effects on stomatal resistance we use the expression Easterling et al. (1992; see Eq. (2) above) as implemented in SWAT (the alternative formulation of Wu et al. (2012a,b) given in Eq. (3) could also be used here).

Canopy resistance has a seasonal component that depends on *LAI*. The correction to *LZETP* factors (which in turn incorporate the seasonal changes in *LAI*) depends only on the ratio of future to current atmospheric CO_2 concentrations, but should be calculated on a month-by-month basis. The correction is estimated by referring to the simplified form of the Penman–Monteith equation known as FAO 56 (Allen et al., 1998), which makes a number of explicit assumptions to replace the resistance terms with a function of wind speed to yield an expression for ET from a reference crop with assumed fixed height and stomatal resistance. In this form, r_c/r_a is replaced by 0.34 u_2, where u_2 is the wind speed at 2 m height (m/s). The reference crop equation was developed under the assumption of a hypothetical short crop of 0.12 m height with albedo of 0.23 and surface resistance of 70 s/m based on a stomatal resistance of an individual leaf of r_l = 100 s/m and *LAI* of 24 times the crop height, and $r_c = r_l/(0.5\ LAI)$. Further, r_a is approximated as $208/u_2$. The effect of changes in CO_2 on AET can thus be calculated by replacing the current condition r_c with Easterling's modified estimate, r_{c1}, in the Penman–Monteith equation. As r_c appears only in the denominator of the Penman–Monteith equation, the ratio can be represented as:

$$\tau = \frac{AET_1}{AET_0} = \frac{\Delta + \gamma r_a + \gamma r_c}{\Delta + \gamma r_a + \gamma r_{c1}}. \tag{7}$$

In this equation,

$$r_{c1} = r_c \Big/ r_c\left(1.4 - 0.4\frac{CO_2}{330}\right). \tag{8}$$

The remaining terms are estimated, following Allen et al. (1998), as:

$$r_c = \frac{r_l}{0.5LAI} = 70, \tag{9}$$

$$r_a = 208/u_2, \tag{10}$$

$$\Delta = \frac{4098 \cdot \left[0.6108 \exp\left(\frac{17.27T}{T+273.3}\right)\right]}{(T + 273.3)^2}, \tag{11}$$

and

$$\gamma = 0.673645 \cdot \left(\frac{293 - 0.0065z}{293}\right)^{5.26}, \tag{12}$$

where T is air temperature (°C) and z is elevation (m).

In Eq. (11), Δ is a function of temperature and will thus change under future climates. However, it would be incorrect to include changes in Δ in the estimation of revised LZETP parameters. This is because the effects of changing temperature on PET via Δ are already incorporated in the Penman Pan PET time series, and varying it here would double-count the effect. Instead, τ should be calculated with Δ set to a single appropriate value for the month in both the numerator and denominator of Eq. (7). Because the intent is to isolate the effect of CO_2 increase from the effect of temperature increase, the monthly calculations of τ are based on current monthly average temperatures. Calculation of τ at higher future temperatures would result in a slightly smaller downward adjustment in *LZETP*.

In sum, the HSPF monthly *LZETP* parameters, representing seasonal adjustments on PET exerted from the lower soil zone, are modified to reflect the relative change in Penman–Monteith reference crop AET expected for increased atmospheric CO_2 concentrations. This will adjust plant transpiration from the soil without modifying the potential rate of evaporation from interception and surface storage.

5. Results

5.1. Comparison of HSPF and SWAT projections under climate change

Both models were applied to the five study areas under baseline and all 14 mid-21st century climate scenarios. Simulations were run for 31 years, with the first year dropped to account for model spin-up (initialization). Results are in a broad sense similar between the two models, but also show some consistent differences.

The initial results were generated with the models in default mode, in which SWAT adjusts for increased CO_2 in future, but HSPF does not. Fig. 2 compares HSPF and SWAT simulated changes in mean annual streamflow at the downstream station of each of the five study areas (expressed as a percent of the baseline results). In general, the mean annual streamflow results provided by the two models are similar, although the SWAT-predicted total streamflow volumes tend to be higher than HSPF. Most notably, in the Minnesota River SWAT predicts substantially higher streamflows relative to HSPF under projected future wetter conditions.

Table 3 compares statistics of the HSPF and SWAT results at the downstream station. Three types of tests are summarized. The first

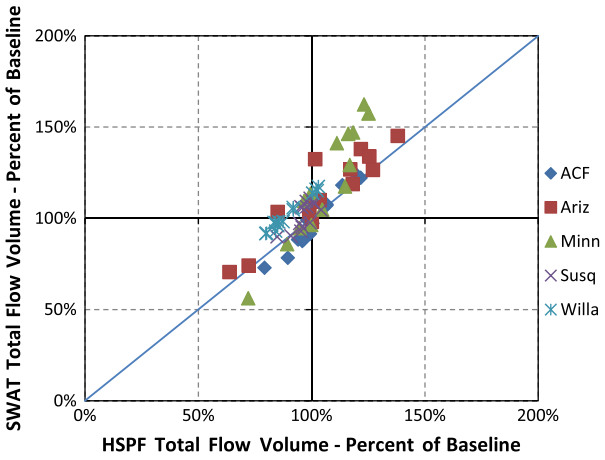

Fig. 2. SWAT and HSPF simulated changes in total streamflow (expressed relative to current conditions). *Note:* Results are for SWAT and HSPF in default mode, in which SWAT accounts for increased atmospheric CO_2 and HSPF does not.

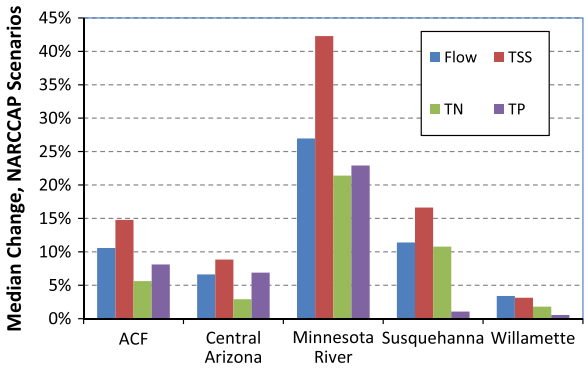

Fig. 3. Simulated effect of changes in atmospheric CO_2 concentration on selected streamflow and water quality endpoints using SWAT; median across six NARCCAP scenarios for mid-21st century. *Note:* Figure shows the median of percent change across 6 future climate scenarios and two land use scenarios in which percent change is calculated as (future – baseline)/baseline.

is a Student's *t*-test on the series of paired means (HSPF and SWAT for each climate and land use scenario), which has a null hypothesis that the mean of the differences between the series is not significantly different from zero. The second test is a two-way ANOVA that looks at choice of watershed model (HSPF or SWAT) as blocks and climate scenario as treatment. The null hypotheses for this test are that the difference between series for a given source of variance is zero. The third test is a linear regression on SWAT results as a function of HSPF results. Where the models are in full agreement, the intercept of such a regression should not be significantly different from zero and the slope should not be significantly different from unity.

The two models produce similar results for mean annual flow with a high Pearson correlation coefficient. The null hypothesis from the *t*-test that the mean difference is zero cannot be rejected. However, the two-way ANOVA shows that both the choice of watershed model and the climate scenario are significant sources of variability in streamflow, with probability values (*p*-value) well below 0.1%. These results suggested that the SWAT and HSPF results are similar in the aggregate, but may contain an underlying systematic shift. This is shown in the regression analysis, where the 95% confidence interval for the regression of SWAT on HSPF does not overlap 1.0 and that for the intercept does not overlap zero.

The water quality results show a wider spread and greater uncertainty. Differences appear to be primarily due to model choice as the ANOVA *p*-value for climate is near 1, but the slope of SWAT versus HSPF results is not significantly different from 1.

5.2. Comparison of SWAT projections with and without effects of increased CO_2

To assess the sensitivity of model results, we performed sets of SWAT simulations with and without increased atmospheric CO_2 for all five study areas using the six NARCCAP dynamically downscaled climate scenarios, which provide internally consistent, downscaled time series of all meteorological variables (the available BCSD scenarios did not include downscaled estimates of relative humidity, solar radiation, or wind). Fig. 3 shows selected flow and water quality endpoints simulated with and without effects of CO_2 concentration changes (see USEPA, 2013 for details). When representing response to increased CO_2 concentrations, the model predicts increased annual streamflow, with median increases by station ranging from 3% to 38%, and an overall median increase of 11%. The overall increase is in the same range as the experimental ecosystem observations summarized by Leakey et al. (2009).

The simulations also suggest increased CO_2 may result in increased pollutant loads, primarily due to the effects of increased streamflow: Loads of TSS show increases from 3% to 57%, with a median of 15%; TP loads increase from zero to 29%, with a median of 6%; and TN loads increase from zero to 34%, with a median of 6%. The large increases in TSS load indicate that the effects of higher runoff under increased CO_2 (largely due to greater soil moisture prior to rainfall events) may outweigh benefits associated with increased residue cover simulated by the model. Nutrients load increases are less than both the streamflow and TSS increases. This is possibly due to increased CO_2 allowing greater plant growth per unit of water, resulting in greater uptake and sequestration of

Table 3
Statistical comparison of HSPF and SWAT outputs at downstream station across all climate scenarios.

Measure	Mean annual streamflow (cfs)	TSS load (t/yr)	TP load (t/yr)	TN load (t/yr)
Paired t-test on sample means				
HSPF mean	20,546	2,398,714	2748	35,346
SWAT mean	20,435	2,865,178	3344	43,275
Pearson correlation	0.989	0.733	0.644	0.948
t-Statistic	0.616	−3.123	−4.783	−7.385
p (two-tail)	0.539	0.002	<0.001	<0.001
Two-way ANOVA on watershed model and climate scenario				
p Value – model	<0.001	0.071	0.006	0.044
p Value – climate	<0.001	0.960	0.999	1.000
Linear regression; SWAT result as a function of HSPF result				
Intercept	1261.7	141,717	954.0	−1173.1
Intercept, 95% confidence	695–1828	−363,064–646,498	431–1477	−4194–1848
Slope	0.933	1.136	0.870	1.257
Slope, 95% confidence	0.911–0.956	0.964–1.307	0.702–1.038	1.189–1.326

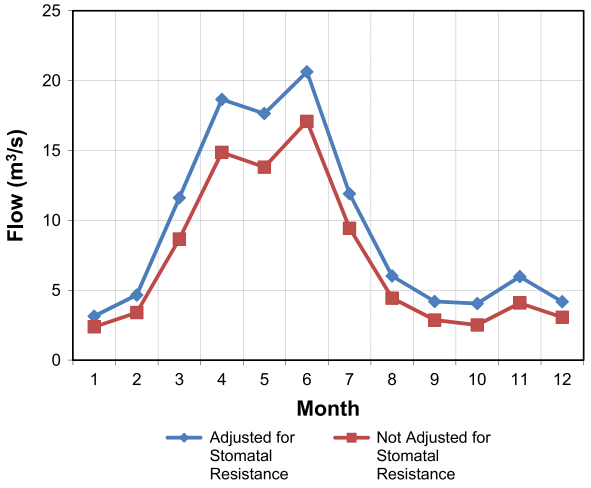

Fig. 4. Monthly average streamflow simulated by SWAT with and without the impact of increased CO_2 on evapotranspiration, Redwood River, MN. *Note:* Results shown are for the cgcm3_CRCM 2050 climate scenario (W1 in USEPA, 2013).

nutrients, and thus smaller increases in nutrient loads relative to streamflow and TSS.

The response to increased atmospheric CO_2 varies greatly by study area, with the greatest effect simulated by SWAT for the Minnesota River basin and the smallest effect for the Willamette basin. Fig. 4 shows the large effect in the Minnesota River basin projected for the NARCCAP mid-21st-century simulation using the Third Generation Coupled Global Climate Model (CGCM3; Environment Canada, 2010) dynamically downscaled with the Canadian Regional Climate Model (CRCM; Environment Canada, 2010). Similar results are seen for the other five NARCCAP scenarios. The effect is relatively large apparently because the land in this basin is predominantly in high-biomass corn-soybean rotation agricultural cropland with precipitation and ET in approximate balance. In contrast the Willamette basin is dominated by evergreen forest and has a moisture surplus for much of the year. In all basins, the CO_2 adjustments in SWAT lead to increased streamflow volumes.

5.3. Comparison of HSPF projections with and without effects of increased CO_2

The strong response to increased CO_2 simulated by SWAT motivated the development of similar adjustments for HSPF. This exercise also reveals important insights into how the ET representation in SWAT might be improved.

5.3.1. Calculating the adjusted parameters for HSPF

The methods described in Section 4 were applied to develop monthly adjustment factors for LZETP in the ACF and Minnesota River models under an increase from the SWAT baseline of 330 ppmv to 527 ppmv CO_2, representative of circa 2050 conditions under both the A2 and A1B emissions scenarios. Details from the ACF model are shown for example, calculated using data from Atlanta, GA. Assuming an elevation of 313 m, $\gamma = 0.06494$ kPa/°C, while the increase in CO_2 yields $r_{c1} = 91.667$.

Δ and r_a are estimated from existing monthly climate normals for air temperature and wind at elevation $z = 10$ m above ground, assuming a logarithmic profile where $u_2 = u_z \cdot 4.87/[\ln(67.8 z - 5.42)]$. Estimates were interpolated to the first of each month consistent with the way that HSPF assigns the monthly parameters (Table 4). LZETP values at the start of each month were constrained to be at least 0.01.

Table 4
Monthly parameters for adjustment of the LZETP parameters in HSPF for 2050 atmospheric CO_2 (ACF Model, calculated at Atlanta).

Month	u_2 (m/s)	T (°C)	Δ	r_a	τ
January	3.34	6.69	0.068	62.21	0.901
February	3.51	7.06	0.069	59.25	0.899
March	3.68	10.28	0.084	56.55	0.902
April	3.51	14.42	0.106	59.25	0.913
May	3.18	18.72	0.135	65.48	0.926
June	2.84	22.94	0.169	73.19	0.939
July	2.67	25.78	0.196	77.76	0.946
August	2.51	26.36	0.202	82.94	0.950
September	2.51	24.50	0.184	82.94	0.947
October	2.84	20.03	0.145	73.19	0.934
November	3.01	14.50	0.107	69.12	0.921
December	3.18	9.67	0.081	65.48	0.909

The LZETP adjustment factors (τ) in Table 4 are dependent on the assumption in Eq. (2) that a doubling of CO_2 leads to a 40% decrease in stomatal conductance. If instead it was assumed that only a 20% decrease in stomatal conductance occurred, the adjustment factors would range from 0.953 to 0.978. The resulting factors represent slightly less than half of the total adjustment at the 40% response level, reflecting the non-linear nature of Eq. (8).

Additional experiments comparing the PET series generated with full climatological data to degraded series in which selected inputs to the Penman–Monteith PET calculation are not updated indicated the importance of including these additional variables (results not shown; see USEPA, 2013). Dew point temperature (which tends to increase in future, warmer climates) has the biggest impact. Including climate model-simulated dew point that is consistent with the scenario temperature and precipitation regime results in a reduction in estimated annual PET of about 11% across all the meteorological stations used for the five study areas. The effect appears to be greater at higher latitudes. The reduction in PET from including simulated dew point is around 10–20% for the Minnesota, New York, Oregon, and Pennsylvania stations, but only 3–10% for the Alabama, Arizona, Florida, and Georgia stations. Omission of solar radiation or wind speed results from the climate scenario appears to have a lesser impact on the estimated PET.

5.3.2. Impacts on hydrology

As expected, implementation of the changes in the *LZETP* parameter results in an increase in total streamflow volume

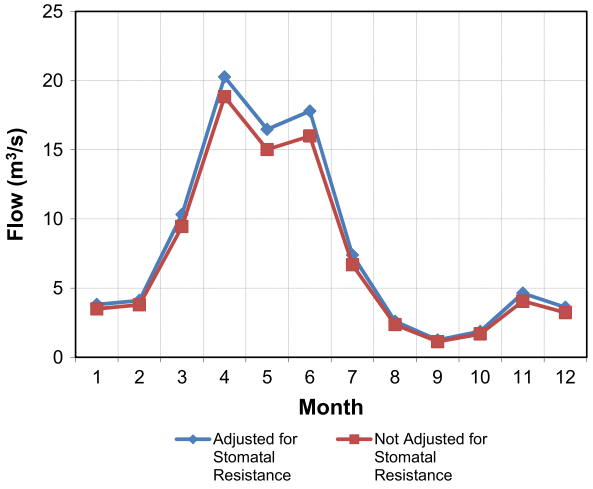

Fig. 5. Change in monthly average streamflow simulated by HSPF after accounting for the impact of increased CO_2 on evapotranspiration in HSPF, Redwood River, MN. *Note:* Results shown are for the cgcm3_CRCM 2050 climate scenario (W1 in USEPA, 2013).

predicted by HSPF. Results were generated at multiple stations for six future climate scenarios, but the effects of CO_2 adjustment are generally consistent between climate scenarios and stations. Typical results for the Redwood River, a HUC 8-digit scale tributary to the Minnesota River, are shown in Fig. 5. Land use in this watershed is predominantly agriculture in corn–soy bean rotation. The *LZETP* adjustment results in a net increase in predicted streamflow of 9.3% (future flow with *LZETP* adjustment minus future flow without adjustment, divided by future flow without adjustment) as an average across the six NARCCAP scenarios, most of which occurs in the spring. The predicted increase in response to CO_2 adjustment is smaller and more seasonally focused than the average 26.9% increase predicted by SWAT (compare Fig. 4). Across nine HUC 8-digit scale analysis points in the Minnesota River basin, the average increase in streamflow after adjusting the *LZETP* parameter is 8.0%, with a range from 5.0% to 9.5%.

In the ACF basin the predicted response is much less than in the Minnesota River basin (as was also predicted by SWAT). Typical results, for Ichawaynochaway Creek (predominantly forested land use) are shown Fig. 6. The average increase in streamflow across all six NARCCAP scenarios predicted by HSPF is 3.2%, while SWAT predicted in average increase of 9.8%. Over ten HUC 8-digit scale analysis points, the average HSPF-predicted increase in total streamflow in the ACF basin was 3.4%, with a range from 2.0% to 5.0%; for SWAT, the average predicted increase in total streamflow was 10.3%, with a range from 8.0% to 12.8%. Results in both study areas are compared in Fig. 7.

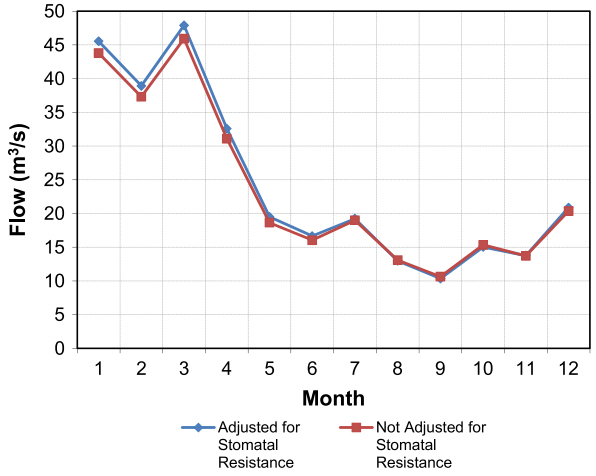

Fig. 6. Change in monthly average streamflow after accounting for the impact of increased CO_2 on evapotranspiration in HSPF, Ichawaynochaway Creek, GA. *Note:* Results shown are for the cgcm3_CRCM 2050 climate scenario (W1 in USEPA, 2013).

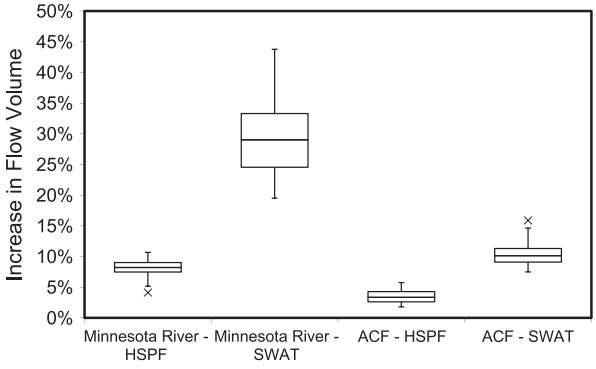

Fig. 7. Increase in total streamflow volume after simulating stomatal response to increased atmospheric CO_2 in HSPF and SWAT. *Note:* Results summarize output for reach HUC8 within a study area over six NARCCAP dynamically downscaled climate scenarios for the mid-21st century (see Johnson et al., 2012 for details) based on a 30-year simulation period. The central line shows the median result, while the box displays the interquartile range. The whiskers are set at the range of the data or 1.5 times the interquartile range, whichever has smaller magnitude. Points outside ± 1.5 times the interquartile range are shown individually.

5.3.3. Impacts on water quality simulation in HSPF

Representing the effects of increased atmospheric CO_2 in HSPF leads to increases in projected runoff and streamflow, which in turn increases predicted pollutant loads (Table 5). Relative increases in TSS transport are greater than increases in streamflow because the models simulate channel erosion (as a function of shear stress) in addition to upland sediment loading. TSS yield relative to streamflow is much less in the lower ACF because of the many upstream impoundments. Unlike SWAT, HSPF does not include a plant growth model and will not represent changes in biomass accumulation associated with altered CO_2, which may in turn influence streamflow and nutrient cycling.

In sum, the revised HSPF model shows an increase in total streamflow volume and pollutant loads in response to the CO_2 effect on plant transpiration. As with SWAT, the effect is greater in the Minnesota River basin than in the ACF basin. However, the HSPF simulations predict a much smaller increase in streamflow volume due to this effect than does SWAT (Fig. 7). The potential reasons for this difference are discussed in Section 6.

6. Discussion: Differences between HSPF and SWAT representation of the effects of increased CO_2

We developed and successfully implemented a method to incorporate effects of increased CO_2 concentrations and resulting changes in stomatal conductance and plant transpiration within the HSPF model. The approach appears to work well, although actual changes in transpiration from specific land cover types could well differ from the simplified predictions in the equation of Easterling et al. (1992).

The projected changes in streamflow and pollutant loading with HSPF after accounting for the CO_2 effect are small, and substantially less than those predicted using the SWAT watershed model. There appear to be two major reasons why the magnitude of the effect is smaller in the HSPF model than in the SWAT model: use of curve number hydrology in SWAT versus infiltration in HSPF, and differences in how CO_2 adjustments in the two models treat the evaporation versus transpiration components of ET.

Several other important feedback loops, other than the CO_2 effect, that have the potential to influence model predictions for hydrology and pollutant loads under a changed climate are also included in the SWAT plant growth model and may merit further investigation:

- Planting, tillage, fertilization, and harvest timing for crops (and start and end of growth for native plants) can be represented by heat unit scheduling, allowing automatic adjustment to a changed temperature regime.
- Evapotranspiration is simulated with the full Penman–Monteith method, allowing dynamic consideration of leaf area development and crop height, instead of via a reference crop approach.
- Plant growth rates vary as a function of temperature, light, water, and nutrient availability.
- Organic matter residue accumulation and degradation on the land surface are dynamically simulated.
- Variations in land surface erosion as a function of leaf and litter cover are dynamically simulated.

Table 5
Differences in predicted average annual pollutant loads after accounting for increased CO_2 in HSPF simulations.

	Minnesota River at Mouth			Apalachicola River at Mouth		
	No CO_2 Adjustment	With CO_2 Adjustment	Change (%)	No CO_2 Adjustment	With CO_2 Adjustment	Change (%)
Flow (m^3/s)	223.6	241.2	7.9	746.2	775.4	3.9
TSS (MT/yr)	1,501,691	1,671,795	11.3	1,477,050	1,562,914	5.8
TP (MT/yr)	2477	2707	9.3	3590	3731	3.9
TN (MT/yr)	48,003	51,743	7.8	13,028	13,840	6.2

6.1. Treatment of evaporation versus transpiration

The SWAT model, in the default mode that is typically applied, uses a curve number approach to estimate direct runoff (SCS, 1972). As stated in the SWAT theory manual (Neitsch et al., 2005), "The amount of water entering the soil profile is calculated as the difference between the amount of rainfall and the amount of surface runoff". Garen and Moore (2005) point out that this approach incorrectly equates curve number runoff (which predicts the rapid response or non-baseflow portion of streamflow) with direct surface runoff. The approach also does not explicitly represent storage by canopy interception. In contrast, the HSPF models for these basins simulate a significant percentage of the total annual precipitation volume going to canopy interception, which is subject to evaporation without stomatal control.

There is another conceptual limitation in the way in which SWAT implements the Penman–Monteith approach to ET. Specifically, SWAT calculates PET from plants using the FAO 56 Penman–Monteith approach (Allen et al., 1998), with correction for CO_2, but then estimates the total ET from all sources (including direct soil evaporation and snow sublimation) as limited to this plant-based estimate of PET. This is incorrect when applied to environments with increased CO_2 concentrations because all ET components are reduced, including those that are not affected by changes in the behavior of leaf stomata. The relevant model code is unchanged in the recent updates of SWAT2012 (rev. 591, released April 15, 2013; http://www.swat.tamu.edu/software/swat-model/). It is therefore likely that the SWAT approach overestimates the fraction of ET that is mediated by plant root uptake, and thus subject to reduction due to reduced stomatal conductance.

HSPF may also be affected by conceptual shortcomings in the treatment of ET. As noted in Section 5.1, plant transpiration from the root zone is simulated only after PET is allocated to active groundwater discharge, interception storage, and upper zone soil storage (as well as to active groundwater storage in wetlands). This prioritization scheme implies that no plant transpiration occurs during periods when the combined evaporation that can be obtained from these stores exceeds PET – which is not entirely correct if plants maintain open stomata to obtain CO_2.

Together, these factors suggest that SWAT likely over-estimates the reduction in ET due to increased CO_2. On the other hand, HSPF may under-estimate the reduction in ET due to the prioritization scheme that allocates PET first to moisture stores other than the soil root zone.

6.2. Implications for model selection

Previous comparison of simulations using SWAT and HSPF show that each model is capable of performing within commonly accepted accuracy standards for watershed models and the two models generally yield similar qualities of fit to observed streamflow and inferred monthly load time series (Johnson et al., 2012). SWAT is able to represent influences of increased atmospheric CO_2 and other feedback responses of plant growth to climate change, while HSPF does not directly represent this feedback. It is unclear, however, how well SWAT is able to represent the complex processes affecting plant growth, nutrient dynamics, and water budgets under changing climate. For example, as CO_2 levels increase, leaf level reductions in stomatal conductance and ET may be offset by increased plant growth and leaf area (as discussed by Wu et al., 2012a,b; Luo et al., 2013). The effects of changes in atmospheric CO_2 on plant growth may also be altered over time due to nutrient limitation (Reich et al., 2006). In addition, SWAT (as implemented here, using version SWAT2005) is less than ideal for assessing water quality response to climate change for a variety of reasons, including simplified simulation of direct runoff using a curve number approach, erosion prediction with MUSLE that does not fully incorporate changes in energy that may occur with altered precipitation regimes, and a simplistic representation of channel erosion processes that appears unlikely to provide a firm foundation for simulating channel stability responses to climate change.

This paper provides an approach to modify the parameters of HSPF to account for the effects of increased CO_2 on transpiration. Application of this approach yields estimated increases in streamflow under higher CO_2 concentrations, but the increases are only about one-third of those predicted by SWAT. As noted above, SWAT assumes that all ET sources (rather than just plant transpiration) are modified by increased atmospheric CO_2. On the other hand, the HSPF model, even if it is appropriately adjusted for decreasing stomatal conductance, does not have the capability of directly simulating the various changes in plant growth, litter production and decomposition, and soil chemistry that are likely to occur under altered climate conditions.

These considerations suggest that a new watershed model formulation, combining a plant growth model (as in SWAT) with a more detailed hydrologic simulation (as in HSPF) may be useful for evaluating watershed responses to climate change, although at the cost of greater model complexity. More complete representation of watershed processes known to be important is also consistent with the general goals of scenario analysis; to explore system sensitivity, identify unexpected or counterintuitive results, and capture the full range of potential outcomes in response to plausible but uncertain future climate conditions.

The issue of plant response to future CO_2 is frequently not addressed in models of watershed response to climate change. The literature includes numerous examples of use of the Precipitation-Runoff Modeling System (PRMS; Leavesley et al., 1983) and the Variable Infiltration Capacity (VIC) model (Gao et al., 2009) to predict watershed hydrology responses to climate change (e.g., Hay et al., 2011; Jung and Chang, 2011; Christensen et al., 2004; Elsner et al., 2010). To date, these studies do not appear to address the effects of increased CO_2. The PRMS model currently does not include an option for a full energy-balance approach to PET, and the work reported by Hay et al. (2011) relied on Jensen-Haise PET based on temperature change alone. Milly and Dunne (2011) pointed out that this approach resulted in estimates of PET that are consistently much greater than predicted by the energy balance in GCMs, resulting in a decrease in runoff with a median of −11% across nine U.S. stream gages and three 2088–2099 climate

projections. The VIC model does implement a form of the Penman–Monteith equation (with canopy resistance set to zero), but does not incorporate an adjustment for increased CO_2 and reduced stomatal conductance. Presumably the VIC model would be amenable to adjustments similar to those proposed above.

Comparison of watershed response to change scenarios using HSPF and SWAT suggests one must also proceed with caution when attempting to estimate even relative aggregate impacts at a national scale through use of models with different underlying formulations. Specifically, the SWAT model incorporation of explicit simulation of plant growth and feedback from CO_2 fertilization has a significant impact on results compared to models that do not simulate this effect. However, comparison of SWAT results to a modified version of the HSPF model that does account for this effect suggests that its magnitude may be over-estimated in SWAT.

7. Conclusions

ET is the largest output term in the water balance of most watersheds. As such, estimation of ET is a crucial component for evaluating watershed response to future climates. Most watershed models use the concept of PET to account for the energy balance that drives ET. Simplified approaches that relate PET solely or primarily to air temperature may be misleading for future climates if other energy balance factors, such as relative humidity, also change. A further complication is imposed by rising concentrations of atmospheric CO_2. Increased CO_2 causes many plant species to reduce stomatal opening, which in turn reduces leaf transpiration, but most watershed models in current use do not account for this effect. The SWAT plant growth model can address CO_2 impacts on transpiration, yielding predictions of lower total ET (and thus smaller reductions or greater increases in summer stream runoff under future climates). Results suggest, however, that the SWAT approach may over-estimate the offsetting effect of increased CO_2 on ET because the algorithm reduces the ET capacity from all sources, including evaporation properly attributed to canopy interception and surface soil storage that is not mediated by plant transpiration.

This paper demonstrates a method that can be used to approximate the changes in the transpiration component of ET (which are affected by stomatal conductance) separately from the changes in the evaporation component in models such as HSPF that do not explicitly model plant growth. Resulting watershed response simulations fall between simulated responses without adjusting for CO_2 impact on plant transpiration and simulations with SWAT that assume that increased CO_2 reduces all components of ET.

Future climates may present a range of challenges to watershed functions. Accurate accounting of the ET component of the water balance is essential to evaluate the potential range of responses. Areas where growing season temperatures will increase will experience increased ET losses and reductions in water availability (relative to general trends in precipitation). The effects of increased CO_2 on plant stomatal conductance will offset some of these changes; however, such offsets only apply to components of ET that are directly mediated by plant transpiration. Thus, simulations of the impacts of climate change on watershed response that project PET based solely on changes in air temperature are likely to under-estimate streamflow and pollutant loads, while simulations that apply a gross CO_2-based correction to all components of ET are likely to over-estimate future streamflow.

Acknowledgments

We thank Debjani Deb, Pushpa Tuppad, and Raghavan Srinivasan of Texas A&M University for developing the SWAT models of the ACF, Minnesota River, and Willamette River watersheds. Jeremy Wyss of Tetra Tech developed the ACF HSPF model, while Brian Bicknell and John Imhoff of AQUA TERRA were responsible for developing the Salt/San Pedro/Verde, Susquehanna, and Willamette HSPF models. Mustafa Faizullabhoy of Tetra Tech processed all the climate scenario data. The writers also thank Seth McGinnis of the National Center for Atmospheric Research (NCAR) for processing the NARCCAP output into change statistics for use in the watershed modeling, as well as the NARCCAP and BCSD project teams. NCAR is supported by the National Science Foundation. The writers acknowledge the modeling groups, the Program for Climate Model Diagnosis and Intercomparison (PCMDI) and the WCRP's Working Group on Coupled Modeling (WGCM) for their roles in making available the WCRP CMIP3 multi-model data set. Support of this data set is provided by the Office of Science, U.S. Department of Energy. Funding for this work was provided by the U.S. Environmental Protection Agency, Office of Research and Development. The views expressed in this paper represent those of the authors and do not necessarily reflect the views or policies of the U.S. Environmental Protection Agency.

References

Alexander, R.B., Smith, R.A., Schwarz, G.E., Boyer, E.W., Nolan, J.V., Brakebill, J.W., 2008. Differences in phosphorus and nitrogen delivery to the Gulf of Mexico from the Mississippi River Basin. Environ. Sci. Technol. 42, 822–830.

Allen, R.G., Pereira, L.S., Raes, D., Smith, M., 1998. Crop Evapotranspiration: Guidelines for Computing Crop Water Requirements. Irrigation and Drainage Paper 56. Food and Agriculture Organization of the United Nations, Rome.

Arnold, J.G., Srinivasan, R., Muttiah, S., Williams, J.R., 1998. Large area hydrologic modeling and assessment. Part 1: Model development. J. Am. Water Resour. Assoc. 34 (1), 73–89.

Bernacchi, C.J., Kimball, B.A., Quarles, D.R., Long, S.P., Ort, D.R., 2007. Decreases in stomatal conductance of soybean under open-air elevation of [CO_2] are closely coupled with decreases in ecosystem evapotranspiration. Plant Physiol. 143, 134–144.

Bicknell, B.R., Imhoff, J.C., Kittle Jr., J.L., Jobes, T.H., Donigian Jr., A.S., 2005. HSPF Version 12.2 User's Manual. National Exposure Research Laboratory, Office of Research and Development, U.S. Environmental Protection Agency, Athens, GA.

Cao, L., Bala, G., Caldeira, K., Nemani, R., Ban-Weiss, G., 2010. Importance of carbon dioxide physiological forcing to future climate change. Proc. Natl. Acad. Sci. USA 107 (21), 9513–9518.

Christensen, N.S., Wood, A.W., Voisin, N., Lettenmaier, D.P., Palmer, R.N., 2004. The effects of climate change on the hydrology and water resources of the Colorado River basin. Clim. Change 62, 337–343.

Crawford, N.H., Linsley, R.K., 1966. Digital Simulation in Hydrology: Stanford Watershed Model IV, Technical Report 39. Department of Civil Engineering, Stanford University, CA.

Duda, P.D., Hummel, P.R., Donigian Jr., A.S., Imhoff, J.C., 2012. BASINS/HSPF: Model use, calibration, and validation. Trans. ASABE 55 (4), 1523–1547.

Easterling, W.E., Rosenberg, N.J., McKenney, M.S., Jones, C.A., Dyke, P.T., Williams, J.R., 1992. Preparing the erosion productivity impact calculator (EPIC) model to simulate crop response to climate change and the direct effects of CO_2. Agric. For. Meteorol. 59 (1/2), 17–34.

Eckhardt, K., Ulbrich, U., 2003. Potential impacts of climate change on groundwater recharge and streamflow in a Central European low mountain range. J. Hydrol. 284 (1–4), 244–252.

Elsner, M.M., Cuo, L., Voisin, N., Deems, J.S., Hamlet, A.F., Vano, J.A., Mickelson, K.E.B., Lee, S.-Y., Lettenmaier, D.P., 2010. Implications of 21st century climate change for the hydrology of Washington State. Climatic Change 102, 225–260.

Environment Canada. 2010. Models: Canadian Centre for Climate Modelling and Analysis. <http://www.ec.gc.ca/ccmac-cccma/default.asp?lang=En&n=4A642EDE-1>.

Ficklin, D.L., Luo, Y., Luedeling, E., Zhang, M., 2009. Climate change sensitivity assessment of a highly agricultural watershed using SWAT. J. Hydrol. 374, 16–29.

Field, C.B., Jackson, R.B., Mooney, H.A., 1995. Stomatal responses to increased CO_2: implications from the plant to the global scale. Plant, Cell Environ. 18, 1214–1225.

Gao, H., Tang, Q., Shi, X., Zhu, C., Bohn, T.J., Su, F., Sheffield, J., Pan, M., Lettenmaier, D., Wood, E.F., 2009. Water-Budget Record from Variable Infiltration Capacity (VIC) Model, Algorithm Theoretical Basis Document. Dept. of Civil and Environmental Engineering, University of Washington, Seattle, WA.

Garen, D.C., Moore, D.S., 2005. Curve number hydrology in water quality modeling: uses, abuses, and future directions. J. Am. Water Resour. Assoc. 41 (2), 377–388.

Gassman, P.W., Reyes, M.R., Green, C.H., Arnold, J.G., 2007. The soil and water assessment tool: historical development, applications, and future research directions. Trans. ASABE 50 (4), 1211–1250.

Gesch, D., Oimoen, M., Greenlee, S., Nelson, C., Steuck, M., Tyler, D., 2002. The national elevation dataset. Photogramm. Eng. Remote Sens. 68, 5–11.
Hay, L.E., Markstrom, S.L., Ward-Garrison, C., 2011. Watershed-scale response to climate change through the twenty-first century for selected basins across the United States. Earth Interact 15, 1–37.
Homer, C., Huang, C., Yang, L., Wylie, B., Coan, M., 2004. Development of a 2001 national landcover database for the United States. Photogramm. Eng. Remote Sens. 70 (7), 829–840.
Homer, C., Dewitz, J., Fry, J., Coan, M., Hossain, N., Larson, C., Herold, N., McKerrow, A., Van Driel, J.N., Wickham, J., 2007. Completion of the 2001 National Land Cover Database for the conterminous United States. Photogramm. Eng. Remote Sens. 73, 337–341.
IPCC (Intergovernmental Panel on Climate Change), 2001. Climate Change 2001: The Scientific Basis. Contribution of Working Group I to the Third Assessment Report of the Intergovernmental Panel on Climate Change (Houghton, J.T., Ding, Y., Griggs, D.J., Noguer, M., van der Linden, P.J., Dai, X., Maskell, K., Johnson, C.A. (Eds.)). Cambridge University Press, Cambridge, UK.
IPCC (Intergovernmental Panel on Climate Change). 2007. Climate Change 2007: Synthesis Report – Summary for Policymakers. Available online at: <http://www.ipcc.ch/pdf/assessment-report/ar4/syr/ar4_syr_spm.pdf> (Accessed 4/1/2013).
Jensen, M.E., Burman, R.D., Allen, R.G. (Eds.), 1990. Evapotranspiration and Irrigation Water Requirements. ASCE Manuals and Reports on Engineering Practice No. 70. American Society of Civil Engineers, NY.
Jha, M., Arnold, J.G., Gassman, P.W., Giorgi, F., Gu, R.R., 2006. Climate change sensitivity assessment on Upper Mississippi River Basin streamflows using SWAT. J. Am. Water Resour. Assoc. 42 (4), 997–1015.
Jiang, T., Chen, Y.D., Xu, C., Chen, X., Chen, X., Singh, V.P., 2007. Comparison of hydrological impacts of climate change simulated in six hydrological models in the Dongjiang Basin, South China. J. Hydrol. 336, 313–333.
Johnson, T.E., Butcher, J., Parker, A., Weaver, C.P., 2012. Investigating the implications of climate change for U.S. stream water quality: The EPA Global Change Research Program's "20 Watersheds" project. J. Water Resour. Plan Manage. 138 (5), 453–464.
Jung, I.-W., Chang, H., 2011. Assessment of future runoff trends under multiple climate change scenarios in the Willamette River basin, Oregon, USA. Hydrol. Process. 25, 258–277.
Karl, T.R., Melillo, J.M., Peterson, T.C. (Eds.), 2009. Global Climate Change Impacts in the United States. Cambridge University Press.
Katul, G.G., R. Oren, S. Manzoni, C. Higgins, Parlange, M.B., 2012. Evapotranspiration: a process driving mass transport and energy exchange in the soil-plant-atmosphere-climate system. Rev. Geophys., 50:RG3002.
Lammertsma, E.I., de Boer, H.J., Dekker, S.C., Dilcher1, D.L., Lotter, A.F., Wagner-Cremer, F., 2011. Global CO_2 rise leads to reduced maximum stomatal conductance in Florida vegetation. Proc. Natl. Acad. Sci. USA 108 (10), 4035–4040.
Leakey, A.D.B., Ainsworth, E.A., Bernacchi, C.J., Rogers, A., Long, S.P., Ort, D.R., 2009. Elevated CO_2 effects on plant carbon, nitrogen, and water relations: six important lessons from FACE. J. Exp. Bot. 60 (10), 2859–2876.
Leavesley, G.H., Lichty, R.W., Troutman, B.M., Saindon, L.G., 1983. Precipitation-Runoff Modeling System: User's Manual. Water-Resources Investigation Report 83-4238. U.S. Geological Survey, Denver CO.
Lopez, A., Fung, F., New, M., Watts, G., Weston, A., Wilby, R.L., 2009. From climate model ensembles to climate change impacts and adaptation: a case study of water resource management in the southwest of England. Water Resour. Res. 45, W08419. http://dx.doi.org/10.1029/2008WR007499.
Luo, Y., Ficklin, D.L., Liu, Z., Zhang, M., 2013. Assessment of climate change impacts on hydrology and water quality with a watershed modeling approach. Sci. Total Environ. 450–451, 72–82.
Maurer, E.P., Brekke, L., Pruitt, T., Duffy, P.B., 2007. Fine-resolution climate projections enhance regional climate change impact studies. EOS. Trans. Am. Geophys. Union 88 (47), 504.
Medlyn, B.E., Barton, C.V.M., Broadmeadow, M.S.J., Ceulemans, R., De Angelis, P., Forstreuter, M., Freeman, M., Jackson, S.B., Kellomäki, S., Laitat, E., Rey, A., Roberntz, P., Sigurdsson, B.D., Strassemeyer, J., Wang, K., Curtis, P.S., Jarvis, P.G., 2001. Stomatal conductance of forest species after long-term exposure to elevated CO_2 concentration: a synthesis. New Phytol. 149, 247–264.
Milly, P.C.D., Dunne, K.A., 2011. On the hydrologic adjustment of climate-model predictions: the potential pitfall of potential evapotranspiration. Earth Interact 15, 1–14.
Monteith, J.L. 1965. Evaporation and the environment. In The State and Movement of Water in Living Organisms. XIXth Symposium, Society for Exp. Biology, Swansea. Cambridge University Press, pp. 205–234.
Najafi, M.R., Moradkhani, H., Jung, I.W., 2011. Assessing the uncertainties of hydrologic model selection in climate change impact studies. Hydrol. Process. 25, 2814–2826.
Nash, J.E., Sutcliffe, J.V., 1970. River flow forecasting through conceptual models, I, A discussion principles. J. Hydrol. 10, 282–290.
Neitsch, S.L., Arnold, J.G., Kiniry, J.R., Williams, J.R., 2005. Soil and Water Assessment Tool Theoretical Documentation, Version 2005. USDA Agricultural Research Service (ARS) Grassland. Soil and Water Research Laboratory, Texas Agricultural Experiment Station, Blackland Research Center, Temple, TX.
Penman, H.L., 1948. Natural evaporation from open water, bare soil, and grass. Proc. R. Soc. Lond. Ser. A 193, 120–146.
Reich, P.B., Hungate, B.A., Luo, Y., 2006. Carbon–nitrogen interactions in terrestrial ecosystem response to rising atmospheric carbon dioxide. Annu. Rev. Ecol., Evol. Syst. 37, 611–636.
SCS, 1972. Section 4: hydrology. In: National Engineering Handbook. Soil Conservation Service, U.S. Department of Agriculture.
Seaber, P.R., Kapinos, F.P., Knapp, G.L., 1987. Hydrologic Unit Maps. Water-Supply Paper 2294. U.S. Geological Survey, Denver CO.
Shiklomanov, A.I., 1998. World Water Resources: A New Appraisal and Assessment for the Twenty-First Century: A Summary of the Monograph "World Water Resources" Report. UNESCO, Paris.
Stockle, C.O., Williams, J.R., Rosenberg, N.J., Jones, C.A., 1992. A method for estimating the direct and climatic effects of rising atmospheric carbon dioxide on growth and yield of crops: Part 1 – Modification of the EPIC model for climate change analysis. Agric. Syst. 38, 225–238.
USDA (United States Department of Agriculture), 1991. State Soil Geographic (STATSG0) Data Base; Data Use Information. Miscellaneous Publication 1492. National Soil Survey Center, Natural Resources Conservation Service, U.S. Dept. of Agriculture, Fort Worth, TX.
USEPA (United States Environmental Protection Agency), 2000. Estimating Hydrology and Hydraulic Parameters for HSPF. BASINS Technical Note 6. EPA-823-R00-012. Office of Water, U.S. Environmental Protection Agency, Washington, DC.
USEPA (United States Environmental Protection Agency), 2008. Using the BASINS Meteorological Database (Version 2006). BASINS Technical Note 10. Office of Water, U.S. Environmental Protection Agency, Washington, DC.
USEPA (United States Environmental Protection Agency). 2009. BASINS 4.0 – Fact Sheet. http://www.epa.gov/waterscience/BASINS/fs-<basins4.html> (accessed January 27, 2010).
USEPA (United States Environmental Protection Agency). 2010. NHDPlus User Guide. Office of Water, U.S. Environmental Protection Agency, Washington, DC. <http://www.horizon-systems.com/nhdplus/documentation.php> (accessed 1/12/2010).
USEPA (United States Environmental Protection Agency). 2013. Watershed Modeling to Assess the Sensitivity of Streamflow, Nutrients, and Sediment Loading to Potential Climate Change and Urban Development in 20 U.S. Watersheds. EPA/600/R12/058F. Mhttp://www.cfpub.epa.gov/ncea/global/recordisplay.cfm?deid=256912> (accessed 10/17/13).
Van Liew, M.W., Feng, S., Pathak, T.B., 2012. Climate change impacts on streamflow, water quality, and best management practices for the Shell and Logan Creek watersheds in Nebraska. Int. J. Agric. Biol. Eng. 5 (1), 13–34.
Williams, J.R. 1975. Sediment-yield prediction with universal equation using runoff energy factor. pp. 244–252 in Present and Prospective Technology for Predicting Sediment Yield and Sources: Proceedings of the Sediment-Yield Workshop, USDA Sedimentation Lab, Oxford, MS, November 28–30, 1972. ARSS-40.
Winchell, M., Srinivasan, R., DiLuzio, M., Arnold, J., 2008. ArcSWAT 2.1 Interface for SWAT2005. User's Guide. Blackland Research Center. Texas Agricultural Experiment Station, Temple, TX.
Wu, Y., Liu, S., Abdul-Aziz, O.I., 2012a. Hydrological effects of the increased CO_2 and climate change in the Upper Mississippi River Basin using a modified SWAT. Climatic Change 110, 977–1003.
Wu, Y., Liu, S., Gallant, A.L., 2012b. Predicting impacts of increased CO_2 and climate change on the water cycle and water quality in the semiarid James River Basin of the Midwestern USA. Sci. Total Environ. 430, 150–160.